Chapter 8

Tie-line Frequency control of Interconnected PV-Wind Hybrid Power system

8.1 Introduction

Photovoltaic (PV) and Wind based generation have experienced tremendous development in recent decade, mainly because of increasing concern for climatic changes and oil prices, which has driven numerous nations to review new technologies to advance Renewable Energy Sources (RES) technology [279]. The power generated from the RES is uncertain as they are related to change in climatic conditions, thereby, the reliable and uninterrupted power supply cannot be extracted from one type RES. However, this can be achieved by the combination of two or more RES selected on the basis of geographical conditions to form a reliable Hybrid power generation. Solar PV and Wind-based power generation are most reliable, promising sources as the solar and wind energy resources are available daily and seasonally. The hybrid PV-Wind power system is gaining importance as a reliable sources of power generation as compared to

conventional generation [280].

The power electronic technology plays a vital role in grid connected distribution generation. During last few years, semiconductor technology has gone tremendous growth with respect to fast operating switches and high power handling capability. The real-time computer-based controller technology which can implement complex control logic in coordination with the power electronic technology have led to the development of efficient and grid responsive converters [281].

8.2 Grid connected PV-Wind hybrid power system

A two-stage grid connected PV-Wind hybrid power system with an improved inverter control is shown in Figure 8.1. A Maximum Power Point Tracking (MPPT) based inverter control is implemented in the

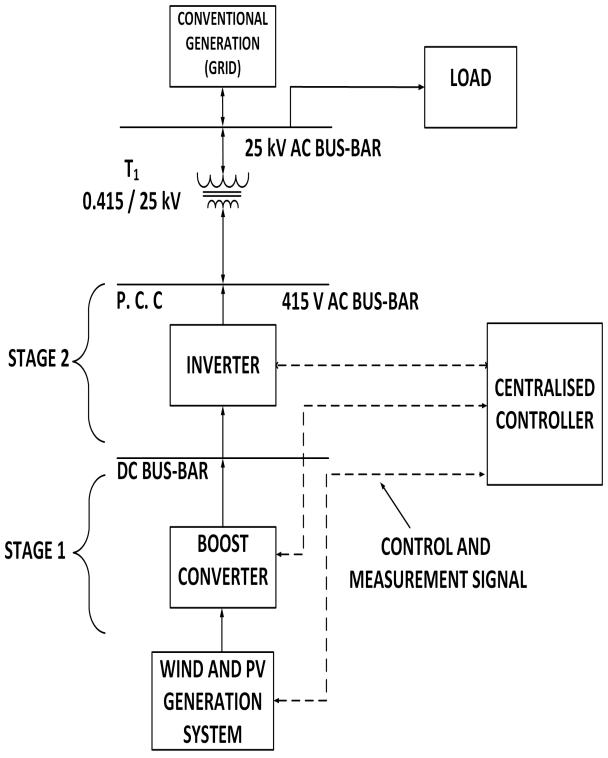

FIGURE 8.1: Block diagram of grid connected PV-Wind hybrid power system

centralized controller as shown in Figure 8.1 to enhance the Maximum Power Point (MPP) tracking and injecting maximum power harnessed into the grid.

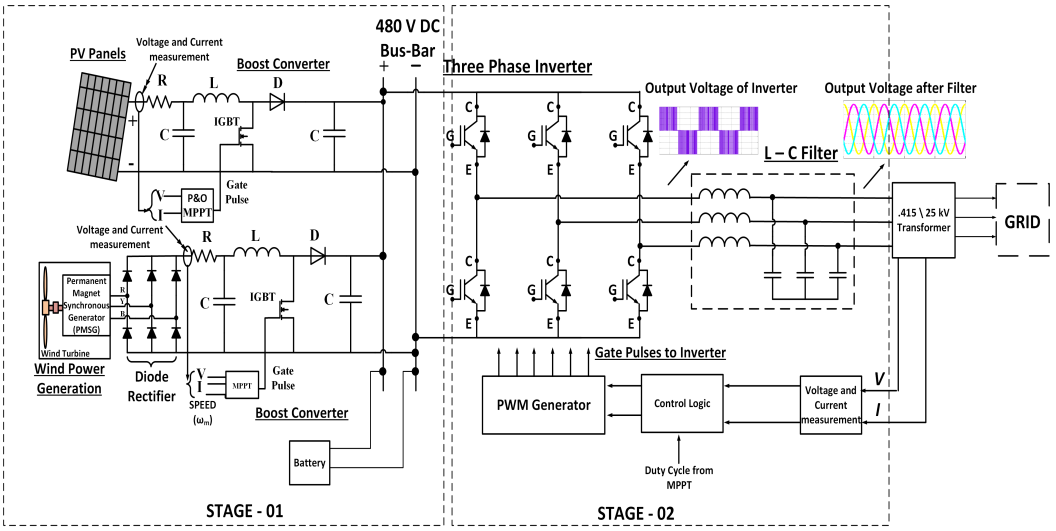

FIGURE 8.2: Circuit level implementation of Grid Connected PV-Wind hybrid power system

A 300 kW PV, 300 kW wind-based generation are implemented in the MATLAB, Simulink. The circuit level implementation is shown in Figure 8.2. The output voltage from PV and Wind generation are connected to a boost converter forming stage-1. The purpose of the stage-1 is to maintain a constant DC voltage irrespective of change in environmental conditions and can be used to harness power at lower solar illumination and wind speeds. The constant DC from stage-1 is connected as an input to Voltage Source Inverter (VSI) which forms stage-2. The stage-2 has to perform DC to AC conversion, grid synchronizing operation, and power injection into the grid. The detailed modeling of PV-wind hybrid power system and control logic implementation will be discussed in detail in the following sections.

8.2.1 Modeling of Stage 1

Stage-1 consists of PV, Wind generation, Boost converter, MPPT algorithm as shown in Figure 8.2. The MATLAB, Simulink implementation and mathematical modeling of PV generation is discussed in detail in Chapter 3 and the equation based modeling of Wind generation consisting of wind-turbine, Permanent Magnet Synchronous Generator (PMSG), diode rectifier and MPPT controlled boost converter is presented in Chapter 4 respectively. The Current (I)-Voltage (V) and Power (P)-Voltage (V) characteristics of PV generation at different solar illumination levels at 25o C operating temperature are graphically represented

in Figure 8.3. A SunPower SPR-415e-WHT-D module data sheet is utilized to simulate one PV panel. Such modules are connected in series and parallel combination to achieve desired output power. The electrical parameters of one module are tabulated in Table 8.1. The simulated power characteristics of the wind turbine at wind speeds are shown in Figure 8.4. The Simulink implementation of MPPT algorithm for PV and the Wind-based generation, modeling of the boost converter [282].

TABLE 8.1: Electrical Parameters of PV Panel

Maximum Power (W) = 414	Cells per module = 128
Open Circuit Voltage V_{oc} (V) = 85.3	Short Circuit Current I_{sc} (A)=6.09
Voltage at MPP V_{mp} (V) = 72.9	Current at MPP I_{mp} (A) = 5.69

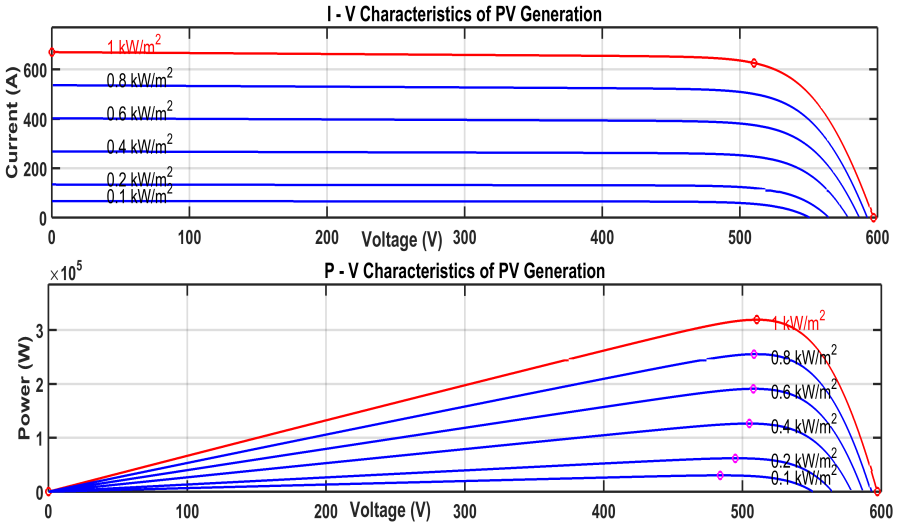

FIGURE 8.3: I-V and P-V Characteristics of PV generation

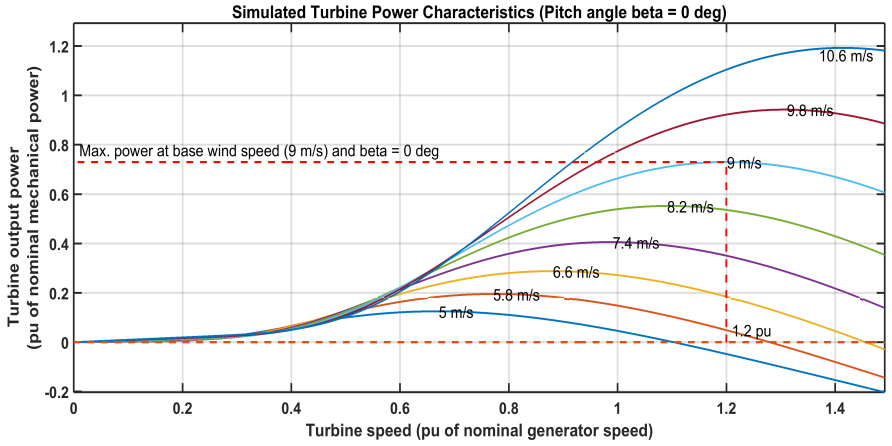

FIGURE 8.4: Simulated Power characteristics of Wind turbine

8.2.2 Modeling of Stage 2:

Stage-2 consists of Voltage Source Inverter (VSI), Inverter, Measurement, grid synchronizing control logic and PWM generator to generate a control signal for VSI. The block diagram representation of proposed MPPT based inverter control technique is shown in Figure 8.5. The inverter has two different control strategies: a voltage regulator and current regulator control. The control technique is implemented in the dq reference frame. The measurement plays an important role in the development of control logic of grid connected inverter as shown in Figure 8.6. A PLL is used to generate reference 'ωt' control signal for grid synchronization.

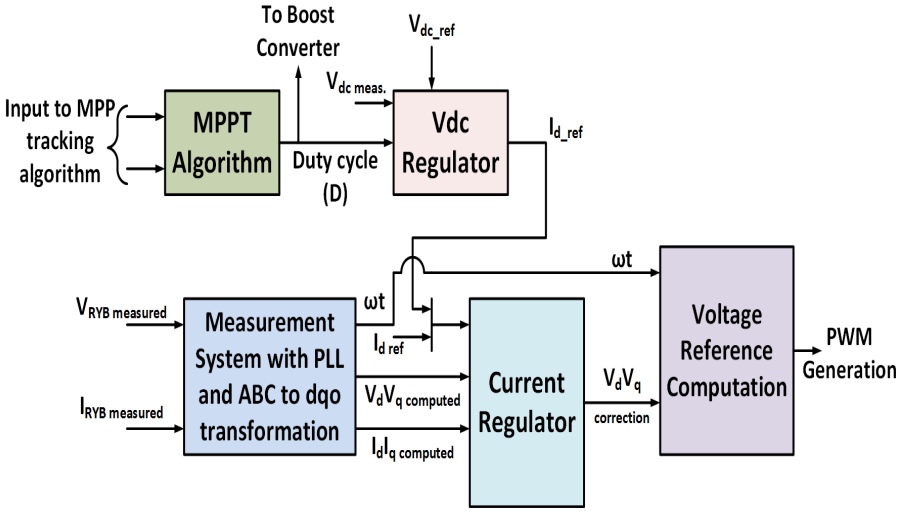

FIGURE 8.5: Block diagram of MPPT based inverter control technique

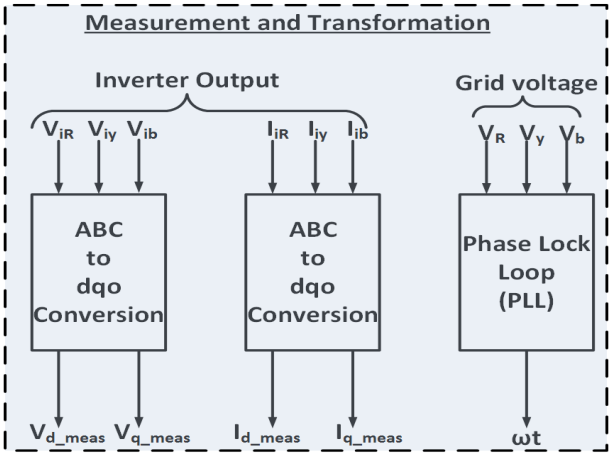

FIGURE 8.6: Measurement and conversion technique

$$\begin{bmatrix} V_{i,RY} \\ V_{i,YB} \\ V_{i,BR} \end{bmatrix} = \begin{bmatrix} R & -R & 0 \\ 0 & R & -R \\ -R & 0 & R \end{bmatrix} \begin{bmatrix} I_R \\ I_Y \\ I_B \end{bmatrix} + \begin{bmatrix} L & -L & 0 \\ 0 & L & -L \\ -L & 0 & L \end{bmatrix} \begin{bmatrix} PI_R \\ PI_Y \\ PI_B \end{bmatrix} + \begin{bmatrix} V_{s,RY} \\ V_{s,YB} \\ V_{s,BR} \end{bmatrix} \tag{8.1}$$

$$\begin{bmatrix} I_{RY} \\ I_{YB} \\ I_{BR} \end{bmatrix} = \begin{bmatrix} 1 & -1 & 0 \\ 0 & 1 & -1 \\ -1 & 0 & 1 \end{bmatrix} \begin{bmatrix} I_R \\ I_Y \\ I_B \end{bmatrix} \tag{8.2}$$

In grid synchronized mode the inverter acts as a voltage controlled current source. The power flow control of the inverter is achieved by controlling V_{d_meas} and V_{q_meas} under synchronous reference frame. V_i, V_s represents the inverter voltage and grid voltage respectively. The power control can be mathematically derived where P in equation (8.1) is time derivative operator. The line to line current can be expressed as equation (8.2) [283].

Substituting (8.2) in (8.1) we have

$$\begin{bmatrix} V_{i,RY} \\ V_{i,YB} \\ V_{i,BY} \end{bmatrix} = Ri \begin{bmatrix} I_{RY} \\ I_{YB} \\ I_{BR} \end{bmatrix} + Li \begin{bmatrix} PI_{RY} \\ PI_{YB} \\ PI_{BR} \end{bmatrix} + \begin{bmatrix} V_{s,RY} \\ V_{s,YB} \\ V_{s,BR} \end{bmatrix} \tag{8.3}$$

where i is the identity matrix and equation (8.3) can be referred in synchronous reference frame as equation (8.4).

$$\begin{bmatrix} V_{id} \\ V_{iq} \end{bmatrix} = \begin{bmatrix} R+L & -\omega L \\ \omega L & R+L \end{bmatrix} \begin{bmatrix} i_{d\_ref} \\ i_{q\_ref} \end{bmatrix} + \begin{bmatrix} V_{sd} \\ V_{sq} \end{bmatrix} \tag{8.4}$$

The angular frequency of the grid is ω in the equation (8.4). The active and reactive power injection into the grid can be controlled by obtaining i_{d_ref} and i_{q_ref}. The values obtained can be submitted in equation (8.4) to find V_{id}, V_{iq} which can be implemented using PWM techniques. In order to have a robust and

accurate control, PI controller is implemented to obtain the V_{id}^*, V_{iq}^* based on the error between the desired and computed active and reactive power.

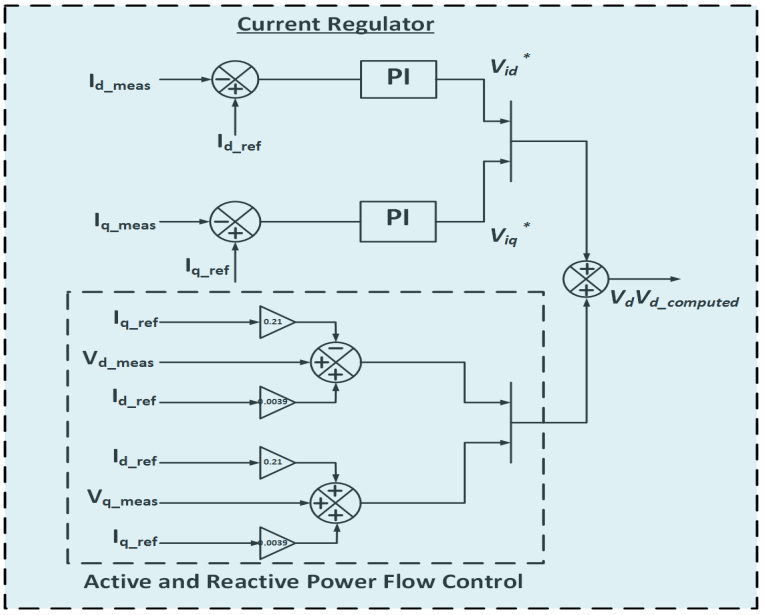

FIGURE 8.7: Current regulator with Active and Reactive power flow control

The block diagram realization of mathematical analysis of current regulator, active and reactive power flow control technique is as shown in Figure 8.7. The values of R = 0.2100 Ω, L = 0.0039 H and PI controller gains for active and reactive power control are K_p = 0.30, K_i = 20.

The block diagram representation of the V_{dc} regulator and voltage reference computation are shown in Figure 8.8, Figure 8.9 respectively. The duty cycle computed by the MPPT algorithm is utilized to

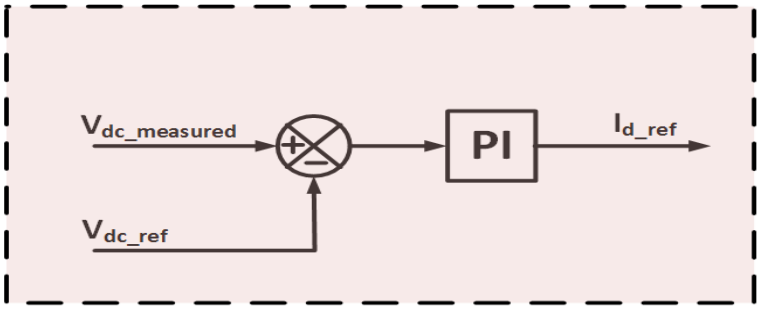

FIGURE 8.8: Block diagram illustration of Vdc regulator

control the duty cycle of the boost converter and the same is utilized to compute I_{dc_ref} as shown in Figure 8.8. The I_{dc_ref} computed is utilized in the modeling of the current regulator, active and reactive power

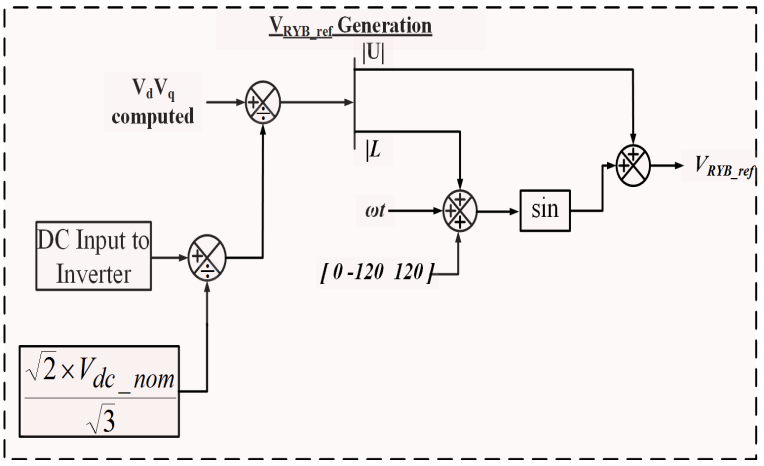

FIGURE 8.9: Block diagram illustration of voltage reference computation

flow control technique as shown in Figure 8.7. The control signal computed from current regulator circuit is then utilized to generate voltage reference signal which is utilized for grid synchronization and the current regulator is utilized for current injection into the grid [284, 285]. The digital simulation of the grid connected PV-Wind hybrid power system and simulation results will be discussed in next section.

8.2.3 System Description and Simulation Results:

A 300 kW PV and 300 kW wind-based generation are implemented in MATLAB, Simulink. The output voltage from the PV and wind are boosted up and maintained constant at desired voltage using MPPT algorithm under varying environmental conditions. The real-time data of solar illumination and wind speed are measured at the location [9, 10]. The voltage source inverter converts DC to AC with the help of proposed MPPT based control technique and grid synchronization is achieved. The MPP tracking of PV and wind generation with the real-time data of solar illumination and wind speed are shown in Figure 8.10,and Figure 8.11 respectively. The amount of power injected into the grid by respective RES with respect to solar illumination and wind speed are plotted in the Figure 8.10, and Figure 8.11 respectively. The dc bus-bar voltage is graphically represented in Figure 8.12. It can be clearly comprehended that the Vdc measured tracks the Vdc reference. From Figure 8.10 to Figure 8.12 it can be concluded that the MPPT algorithm operation is as desired by tracking maximum power from PV and Wind generation under

varying environmental conditions. The computation of I_d and I_q plays a vital role in power flow control of

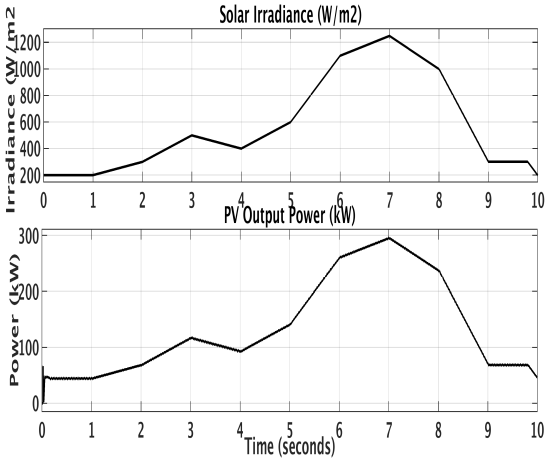

FIGURE 8.10: PV generation with real time data od solar illumination

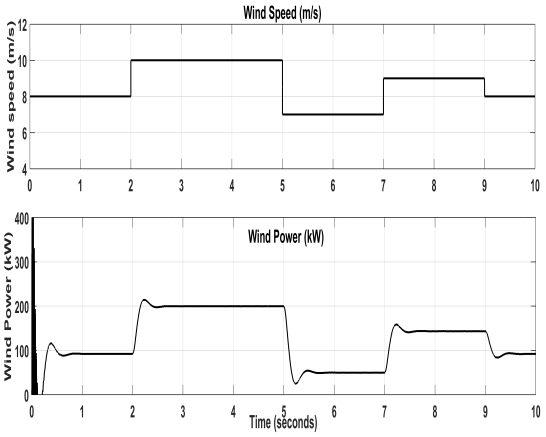

FIGURE 8.11: Wind generation with real time data of wind speed

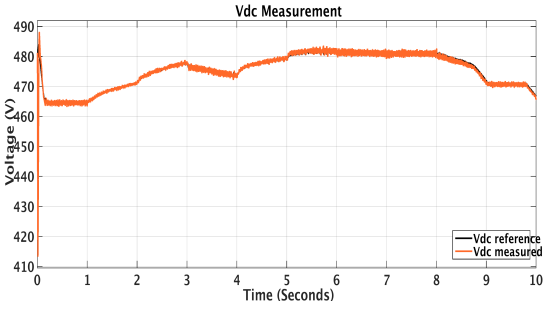

FIGURE 8.12: DC bus-bar voltage

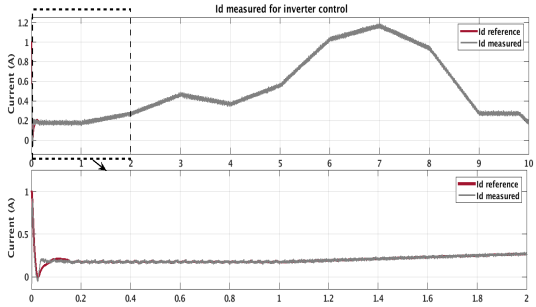

FIGURE 8.13: I_d current for inverter control

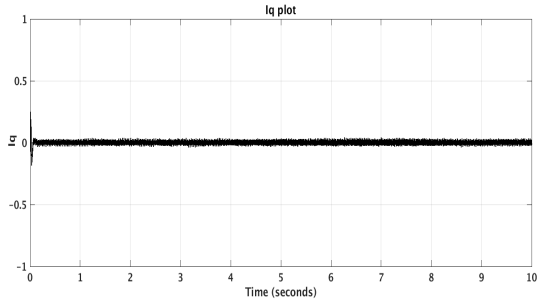

FIGURE 8.14: I_q current for inverter control

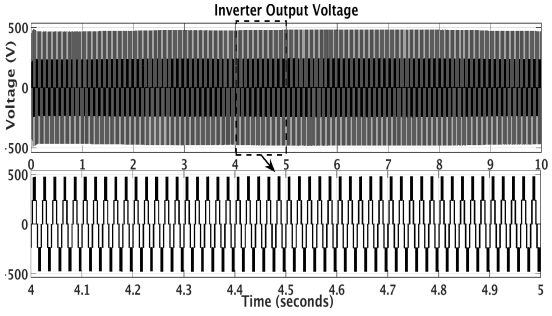

FIGURE 8.15: Simulated Inverter Output Voltage

the inverter. The computational values are compared with the reference values are graphically represented in Figure 8.13, and Figure 8.14 respectively. It can be clearly comprehended that the measured values duplicates the reference values. The initial portion of I_d current is magnified and shown in Figure 8.13. The inverter output voltage is shown in Figure 8.15 and the per phase voltage measured at the 25 kV AC

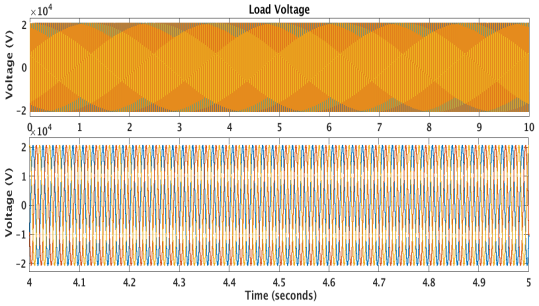

FIGURE 8.16: Simulated Load Voltage

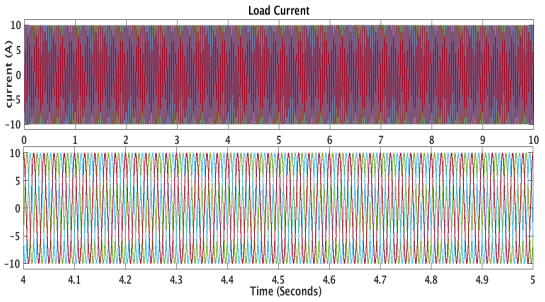

FIGURE 8.17: Simulated Load Current

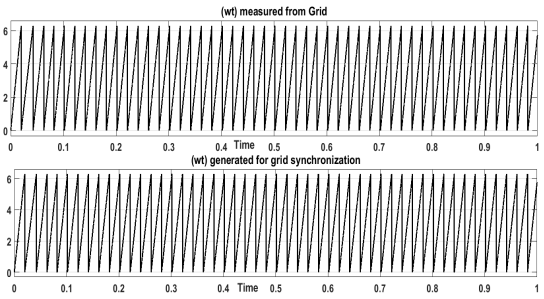

FIGURE 8.18: ωt measured and computed

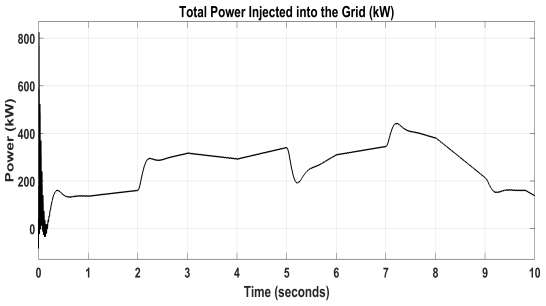

FIGURE 8.19: Total Power Injected into the grid

bus-bar is graphically represented in Figure 8.16 and the load current is plotted in Figure 8.17. The ωt measured from the grid and the ωt generated for grid synchronization and voltage reference computation is shown in Figure 8.18.

The computation of ωt plays a vital role in grid synchronization inverter. If the ωt is not computed in the phase of ωt measured then the computed inverter voltage and frequency will not match that of the grid and the inverter will not be able to synchronize to the grid. From the Figure 8.18, it can be observed that the measured and computed ωt for grid synchronizing inverter are in phase and it can be comprehended from the simulation results that the proposed controller is able to synchronize to the grid and the power generated from the RES is injected into the grid. The total power injected into the grid is graphically represented in the Figure 8.19. Further Tie-line control of interconnected PV Wind hybrid system will be studied.

8.3 Tie-line Frequency Bias Control of Interconnected PV Wind Hybrid Power system

Renewable Energy Sources (RES) are rapidly gaining popularity for clean and green generation and 3-phase grid connection is required. An important aspect in grid integration is the optimal power dispatch and grid integration to the existing power system, where efficiency is primary requirement [286]. In the interconnected power system, Automatic Generation Control (AGC) plays a vital role in ensuring reliability and power quality of the grid. In large scale systems, all the generating units operate at the same frequency as they are synchronized to the power system. Any change in load in the system causes frequency deviation in the area of change and this change in frequency causes the generators synchronized to the system to act according to the change. The power is transferred through tie-line to compensate the change in load [287]. The Load Frequency Control (LFC) problem has gained much importance because of large capacity and complication in the advanced integrated network. The main goal of LFC is to adjust the power generated by the generators such, that the tie-line power and frequency of the power system are kept within the prescribed limits [288]. Different control strategies of LFC of the power system has been proposed and investigated by many researchers in recent years [289–293].

In LFC technique to minimize the frequency error, a PI controller is employed. The PI controller is employed due to its simplicity, easy actualization, cost-effective, rugged and localized behavior of the control strategy [294, 295].

The PI controller reduces the steady-state deviation of the frequency to zero but the dynamic performance of the system is effected. As the dynamic behavior of the system is effected it results in longer settling time of frequency and tie-lime power deviation. In order to overcome the drawbacks of conventional controller various controllers were proposed in the literature such as Fuzzy Logic Controller (FLC), Model Predictive Control (MPC) technique, decentralized coefficient diagram method (CDM), Adaptive Neuro-fuzzy system (ANFIS), effect of Phase Lock Loop (PLL) and frequency measurement on

LFC, dual model BAT algorithm based scheduling of PI controllers, Fuzzy gain scheduling of PI, optimal firefly algorithm, droop characteristics based controller [296, 297].

The LFC / AGC employed in the interconnected system uses tie-line bias control strategy to maintain scheduled power interchange and frequency. The LFC will regulate the generators connected to the tie-line to maintain stability under different load perturbation in any area of the interconnected system. In general, there are three modes in which interconnected operation can be carried out

- **Flat Frequency Control:** The control is to obtain a constant frequency. In this type of control, the generators respond to frequency changes only. It cannot have control over the power flow in the interconnected tie-line.
- **Flat Tie-line Control:** In this method of control implementation the system responds to tie-line changes and changes its generation to maintain the scheduled tie-line interchange. The controller cannot respond to frequency changes.
- **Frequency Bias Control:** Both the above methods have disadvantages. So, as to overcome it a combined control is used, called the Frequency Bias Control. The controller responds to tie-line power and frequency change in the system and changes generation to maintain the stability of the system.

From the literature, it can be observed that no specific research was done towards interconnection of the only RES without any storage device or diesel generator set. All the controllers proposed were investigated by using the transfer function derived from the behavior of the actual system.
With the above drawback, a Tie-Line Frequency Bias Control of Two-Area PV-Wind hybrid power system is investigated with the equation based implementation of PVWHPS and droop characteristics based LFC implementation. A two-area system is considered for the study with each area consisting of 140 kW PV-Wind generation where PV generation is of 100 kW and 40 kW of wind generation respectively. Such

two areas are interconnected through a tie-line. The performance of the tie-line frequency bias controller is investigated for the change in the load of area-2. The block diagram representation of the system is shown in Figure 8.20 and the electrical equivalent of the system is shown in Figure 8.21.

FIGURE 8.20: Two-area system

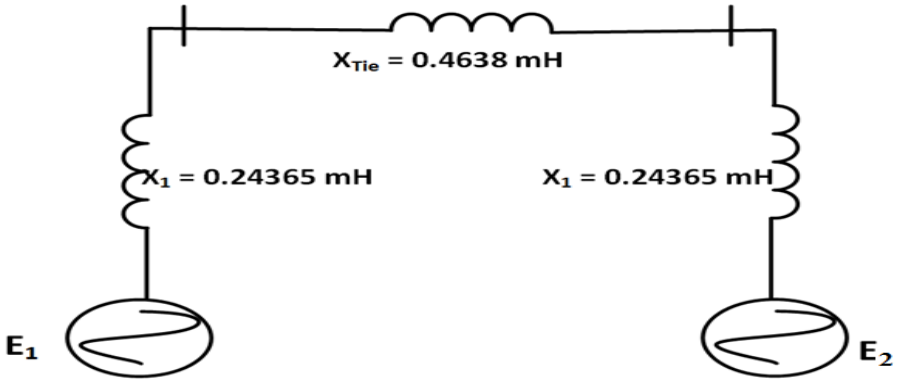

FIGURE 8.21: Electrical equivalent of Two-area system

A flat frequency tie-line bias control is implemented using droop characteristics technique. The generation will respond to change in frequency of the system and will maintain the frequency of the system at 50 Hz. Under steady-state, each area of the two-area system shown in Figure 8.20 are loaded by 100 kW and increase in load demand of 80 kW is observed in the area2. The performance of the controller is analyzed under this condition and the performance is compared with the mathematical analysis of the system. The element-wise representation of PV-wind hybrid power system is shown in Figure 8.22. Further, the droop characteristics design for both areas and mathematical analysis of tie-line controller will be discussed.

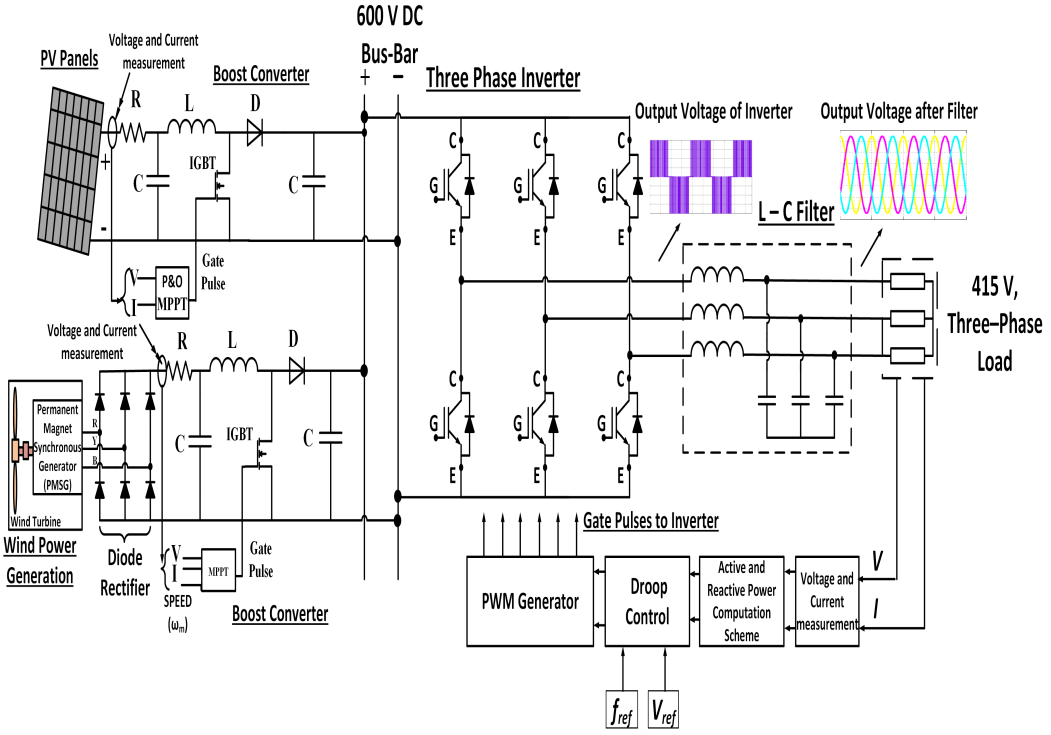

FIGURE 8.22: Element wise representation of hybrid power system

8.4 Droop characteristics design of Inverter:

Area 1: The droop constant R_1 is defined as the ratio of change in frequency (Δf) to the change in output power (ΔP) of the inverter and is taken as

$$R_1 = \frac{\Delta f}{\Delta P} = \frac{0.2}{11} = 0.018 \tag{8.5}$$

The frequency dependent load constant D_1 is 0.8 i.e. The frequency of the system starts decreasing when the load reaches 80% of full load as shown in Figure 8.23. The droop characteristics of the inverter are graphically represented in Figure 8.23

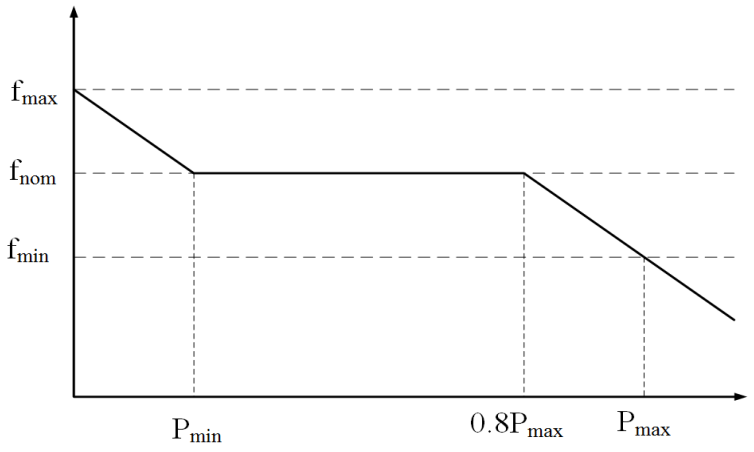

FIGURE 8.23: Droop Characteristics

Area 2: The droop constant R_2 is defined as the ration of change in frequency (Δf) to the change in output power (ΔP) of the inverter and is taken as

$$R_2 = \frac{\Delta f}{\Delta P} = \frac{0.2}{5} = 0.04 \tag{8.6}$$

The frequency dependent load constant D_2 is 1 i.e. The frequency of the system decreasing when the load reaches 100% of full load as shown in Figure 8.24. The droop characteristics of the inverter are graphically represented in Figure 8.24

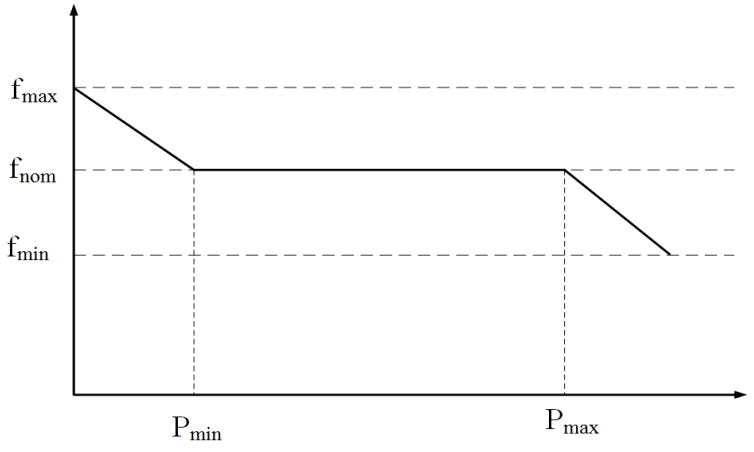

FIGURE 8.24: Droop Characteristics

8.5 Mathematical Analysis:

The tie-line power interchange is 40 kW and change in load is 80 kW. Considering base KVA to be 500 KVA,

Change in load

$$\Delta P_{L2} = \frac{80}{500} = 0.16pu \tag{8.7}$$

$$\Delta\omega = -\frac{0.16}{\beta_1 + \beta_2} \tag{8.8}$$

where,

$$\beta_1 = \frac{1}{R_1} + D_1 = 56.35 \tag{8.9}$$

$$\beta_2 = \frac{1}{R_2} + D_2 = 26 \tag{8.10}$$

$$\Delta\omega = -\frac{0.16}{56035 + 26} = -1.9429 \times 10^{-}3 \tag{8.11}$$

Change in Frequency due to change in load in area 2 is

$$\Delta f = 50 - (-1.9429 \times 10^{-}3 \times 50) = 49.9029Hz \tag{8.12}$$

$$\Delta P_{12} = -\frac{\Delta P_{L1}\beta_2}{\beta_1 + \beta_2} = -0.10927p.u = 54.634kW \tag{8.13}$$

Change in generation of area 1

$$\Delta P_{m1} = -\frac{\Delta\omega}{R_1} = -0.1084pu = -54.2kW \tag{8.14}$$

Change in generation of area 2

$$\Delta P_{m2} = -\frac{\Delta\omega}{R_2} = 0.04878pu = 24.39kW \tag{8.15}$$

Change in load in are 2 due to drop in frequency is

$$-\Delta\omega D_2 = -1.9512 \times 10^{-}3p.u = -0.9756kW \tag{8.16}$$

Change in generation of the system

$$\Delta P_{m1} + \Delta P_{m2} = 54.2 + 24.39 = 78.59kW \tag{8.17}$$

Change in load = 80 - 0.78048 - 0.9756 = 78.24 kW.

8.6 Simulation Results:

The Simulink implementation of the two area system is shown in Figure 8.25 The inverter output line

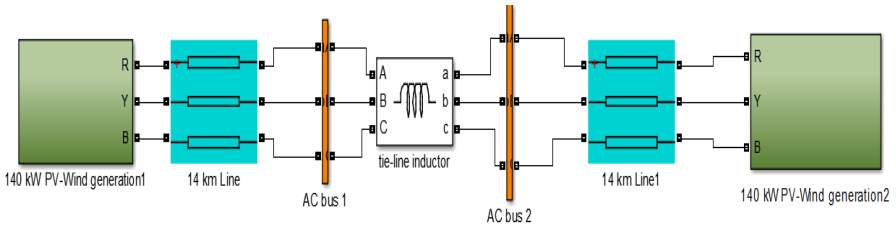

FIGURE 8.25: Simulink Implementation of two-area system

voltage without and with filtering is graphically represented in Figure 8.26. The output voltage, current

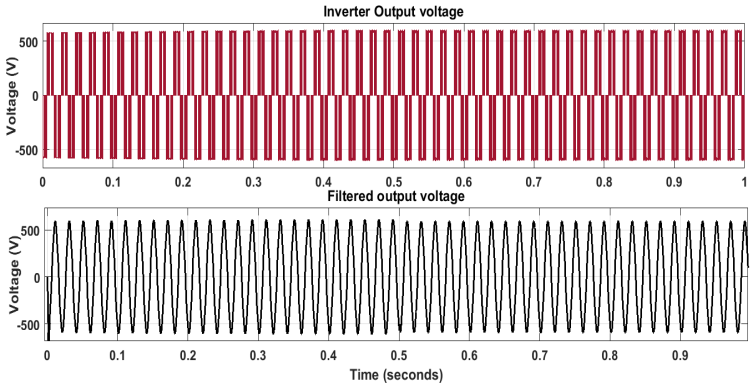

FIGURE 8.26: Inverter output voltage

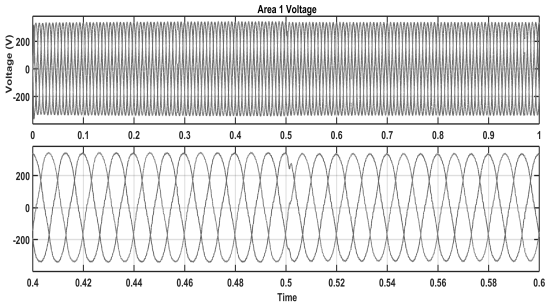

FIGURE 8.27: Simulated Voltage of area 1

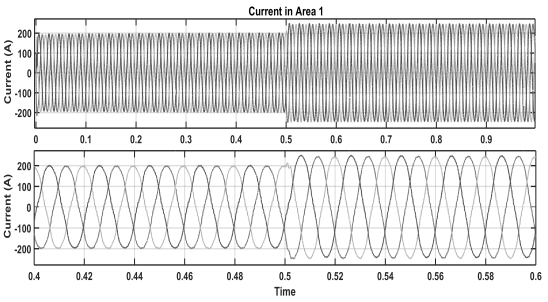

FIGURE 8.28: Simulated Current of area 1

and power of area 1 are graphically represented in Figure 8.27, Figure 8.28 and Figure 8.29.

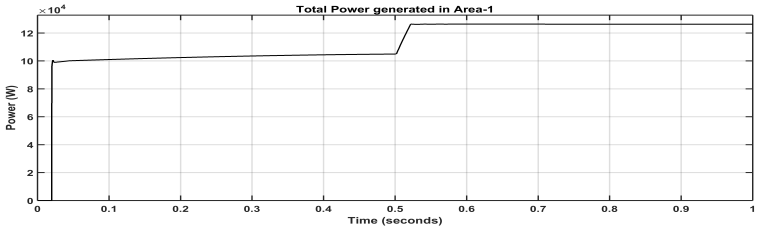

FIGURE 8.29: Power generated in area 1

The output voltage, current and power of area 2 are graphically represented in Figure 8.30 and Figure 8.31. Tie-line Voltage, current and power interchange are graphically represented in Figure 8.32, Figure 8.33

The frequency of the system is plotted in Figure 8.34. From the Figure 8.34 it can be comprehended that the droop characteristics based tie-line control is able to maintain the frequency of the system constant at 50 Hz under steady state and change in load in one of the areas in hybrid power system with proper

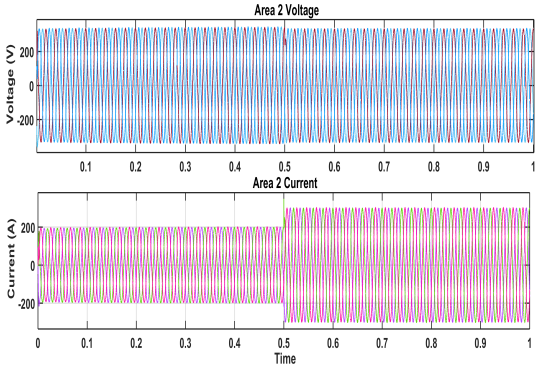

FIGURE 8.30: Simulated Voltage and current of area 2

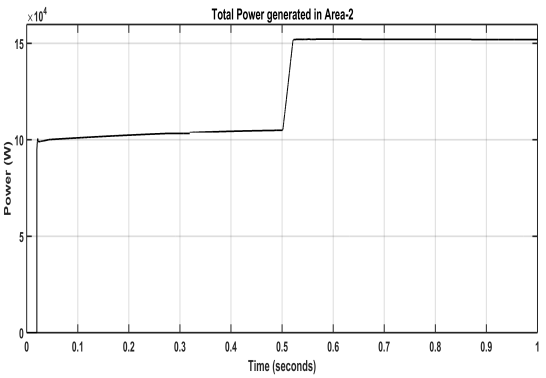

FIGURE 8.31: power generated in area 2

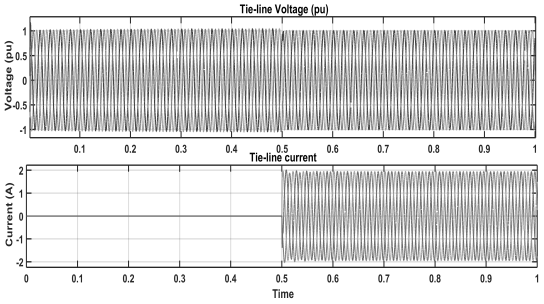

FIGURE 8.32: Simulated Voltage and current of tie-line

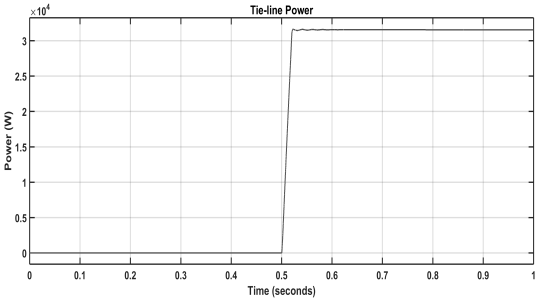

FIGURE 8.33: Tie-line Power interchange

tie-line power exchange. In order to have a clear undersatnding of the control action a comparative

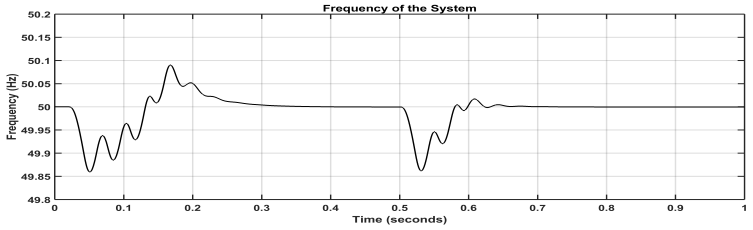

FIGURE 8.34: Frequency of the system

analysis of simulated and mathematical analysis is tabulated in Table 8.2.

TABLE 8.2: A Comparative analysis of mathematical and simulation of two-area system

Parameter	**Mathematical Analysis**	**Simulation Analysis**
Change in Frequency (Hz)	49.9024	49.9409
Power Interchange (kW)	54.634	52.11
Change in Generation in Area 1 (kW)	54.2	52.89
Change in Generation in Area 2 (kW)	24.39	25.4
Decrease in load in Area 2 (kW) due to change in frequency	0.9756	0.97145
Change in Generation (kW)	78.59	78.29
Change in load (kW)	78.24	78.23

8.7 Summary:

In the MPPT based inverter control technique for grid connected PV-Wind hybrid power system is proposed. A mathematical modeling of 300 kW each PV and Wind generation system is presented and detail analysis of proposed controlled technique is represented. The real-time data of solar illumination and wind speed are utilized to emphasize the control action of the controller under varying environmental conditions. The model-based design of the system is implemented in MATLAB, Simulink.

The simulation results demonstrates enhanced control of proposed controller under varying environmental condition by maintaining DC bus bar voltage at desired level. The power generated by the PV and the wind under low solar illumination, wind speed respectively are fed into the grid by maintaining the required output voltage, current, and frequency of the system. The proposed control implementation was able to be grid synchronized under varying environmental conditions and injecting the maximum power extracted from the RES generation.

A tie- line frequency bias control of interconnected PV-Wind hybrid power system was presented. The performance analysis of the droop characteristics implementation is being investigated under load change in one area. A comparative study of the mathematical and simulation analysis is tabulated in Table 8.2. It can be comprehended that the controller action is as desired.